T DOCUMENTATION PAGE

1a. REP NO	AD-A208 894	1b. RESTRICTIVE MARKINGS NONE
2a. SECU NO		3. DISTRIBUTION / AVAILABILITY OF REPORT
2b. DECLASSIFICATION / DOWNGRADING SCHEDULE NONE		UNLIMITED

4. PERFORMING ORGANIZATION REPORT NUMBER(S)	5. MONITORING ORGANIZATION REPORT NUMBER(S)
Technical Report # 29	

6a. NAME OF PERFORMING ORGANIZATION Stanford University	6b. OFFICE SYMBOL (If applicable)	7a. NAME OF MONITORING ORGANIZATION Office of Naval Research

6c. ADDRESS (City, State, and ZIP Code) Department of Chemical Engineering Stanford University Stanford, CA 94305-5025	7b. ADDRESS (City, State, and ZIP Code) 800 North Quincy Avenue Arlington, VA 22217

8a. NAME OF FUNDING / SPONSORING ORGANIZATION Office of Naval Research	8b. OFFICE SYMBOL (If applicable)	9. PROCUREMENT INSTRUMENT IDENTIFICATION NUMBER N00014-87-K-0426

8c. ADDRESS (City, State, and ZIP Code) 800 North Quincy Avenue Arlington, VA 22217-5000	10. SOURCE OF FUNDING NUMBERS			
	PROGRAM ELEMENT NO.	PROJECT NO.	TASK NO.	WORK UNIT ACCESSION NO.

11. TITLE (Include Security Classification)

Ultrathin Poly(methyl methacrylate) Resist Films for Microlithography

12. PERSONAL AUTHOR(S)
S. W. J. Kuan, C. W. Frank, Y. H. Yen Lee, T. Eimori, D. R. Allee, R. F. W. Pease, R. Browning

13a. TYPE OF REPORT	13b. TIME COVERED FROM 88/6/1 TO 89/5/31	14. DATE OF REPORT (Year, Month, Day)	15. PAGE COUNT

17.	COSATI CODES		18. SUBJECT TERMS (Continue on reverse if necessary and identify by block number)
FIELD	GROUP	SUB-GROUP	

19. ABSTRACT (Continue on reverse if necessary and identify by block number)

To improve pattern fidelity of electron beam lithography in the nanometer regime a new class of ultrathin resist (less than 20 nm) has been investigated. Such films can be exposed with very low energy (less than 1 keV) electrons to virtually eliminate proximity effects or, at conventional energies, to allow easier proximity effect correction. In this paper we have investigated the lithographic performance of LB PMMA films with thicknesses ranging from 0.85 nm (one monolayer) to 7.7 nm (nine monolayer) exposed with different electron beam energies. Two types of defects, with sizes less than 20 nm, have be observed in the films after exposure and pattern transfer into chromium. The first type, observed only in films less than seven layers thick, was uniformly distributed over the sample; the second type was only observed around the exposed regions for films thicker than nine layers. Comparisons are made with Monte Carlo simulation.

20. DISTRIBUTION / AVAILABILITY OF ABSTRACT ☑ UNCLASSIFIED/UNLIMITED ☐ SAME AS RPT ☐ DTIC USERS	21. ABSTRACT SECURITY CLASSIFICATION Unclassified
22a. NAME OF RESPONSIBLE INDIVIDUAL Dr. Kenneth J. Wynne	22b. TELEPHONE (Include Area Code) (202)696-4410	22c. OFFICE SYMBOL

OFFICE OF NAVAL RESEARCH

Ultrathin Poly(methyl methacrylate) Resist Films for Microlithography

by

S. W. J. Kuan, C. W. Frank, Y. H. Yen Lee, T. Eimori, D. R. Allee,
R. F. W. Pease and R. Browning

Stanford University
Departments of Chemical Engineering and Electrical Engineering
Stanford, CA 94305

May 30, 1989

ULTRATHIN POLY(METHYLMETHACRYLATE) RESIST FILMS FOR MICROLITHOGRAPHY

S.W.J. Kuan and C.W. Frank -
Department of Chemical Engineering, Stanford University

Y.H. Yen Lee, T. Eimori[a], D.R. Allee, R.F.W. Pease
Department of Electrical Engineering, Stanford University

R. Browning
Center for Intergrated Systems, Stanford University

ABSTRACT

To improve pattern fidelity of electron beam lithography in the nanometer regime a new class of ultrathin resist (less than 20 nm) has been investigated. Such films can be exposed with very low energy (< 1 keV) electrons to virtually eliminate proximity effects or, at conventional electron energies, to allow easier proximity effect correction. In a previous study we investigated ultrathin (14 nm) PMMA films, prepared both by spin casting and Langmuir-Blodgett (L-B) techniques, as high resolution electron beam resists and reported that the pinhole density in 14 nm L-B PMMA films was considerably lower than the density in spin-cast PMMA films of comparable thickness. 45-nm-wide lines were fabricated in 50-nm-thick chromium films using L-B PMMA films as resists. In this paper, we have investigated the lithographic performance of L-B PMMA films with thicknesses ranging from 0.85 nm (one monolayer) to 7.7 nm (9 monolayer) exposed with different electron beam energies. Two types of defects, with sizes less than 20 nm, have been observed in the films after exposure and pattern transfer into chromium. The first type, observed only in the samples with PMMA resist films thinner than 7 layers, was uniformly distributed over the sample and the number of the defects increased dramatically as the films thickness decreased. The second type was only observed around the exposed regions in the films thinner than 9 layers. For the second type, the number of the defects was found to depend on the beam energy and substrate type. Sources of the two types of defects will be discussed and the experimental results will be compared with a Monte-Carlo simulation. It was also demonstrated that 20-nm-wide lines and 160-nm-wide spaces could be achieved in 50-nm-thick chromium films using 7 layer L-B PMMA films as resists.

INTRODUCTION

One limitation of electron beam lithography is the proximity effect[1] caused by the exposure of resist by electrons backscattered from the substrate. This effect constitutes a background on which the pattern is superimposed, which means that the energy dissipated by the electrons at any given point in the resist depends upon the "proximity" of adjacent exposures, thereby reducing the pattern fidelity.

There have been many published correction methods for the proximity effect. Such methods include dose correction,[2] shape correction,[3] and the equalization of the background method (GHOST).[4] A lengthy and costly computation is required for the first two methods and the GHOST method requires additional field exposures, which results in lower image contrast. The idea of using high energy electrons (> 50 keV) to minimize the proximity effect was also proposed by several researchers.[5,6] However, this method does not totally eliminate the proximity effect. In addition, the substrate could be damaged by the high energy electrons.

Using low energy electrons (< 1 keV) for lithography seems to offer a good solution for the elimination of the proximity effect. By using low energy electrons, electron backscatter from the substrate can be minimized or eliminated, thereby reducing the proximity effect. The major limitation in the application of low energy electrons for lithography is that thin resist films (< 100 nm) must be used in order to allow the electrons penetrate the resist. Conventional spin-cast resist films with thickness less than 100 nm usually suffer from the following problems; high pinhole density, inadequate etch resistance and inability to cover the surface topographies. Since there has been only a few studies of the performance of ultrathin resists[7-9], and a thorough study on the resist preparations, resist materials and the electron-resist interactions for ultrathin resists is necessary.

In a previous study,[8] we investigated the possibility of using 14 nm L-B PMMA and spin-cast PMMA films as high resolution electron beam resists. We found that the defect

densities of the 14 nm spin-cast PMMA films are much higher (10^4/cm^2) than that of the 14 nm L-B PMMA films (< 10/cm^2). The etch resistance of these two films is sufficient to protect a 50-nm-thick chromium layer and 45 nm-wide lines were fabricated in 50-nm-thick chromium films using the 14-nm-thick L-B PMMA films as resists. In this investigation we have studied the lithographic performance of L-B PMMA films as a function of film thickness (0.85 nm to 7.7 nm) and exposure beam energy (2.5 keV to 40 keV) on two different substrates. Monte-Carlo simulations also have been performed and compared with the experimental results.

EXPERIMENTAL

A. Materials

Atactic-PMMA obtained from Pressure Chemical, with weight average molecular weight (Mw) of 188,100 and Mw/Mn < 1.08, where Mn is number average molecular weight, was used to prepare the ultrathin electron beam resist films. Spectroscopic grade chloroform, purchased from J. T. Backer, was used to prepare the PMMA solutions.

B. Substrates

Two different substrates have been used in this study. One consists of 50 nm evaporated chromium (Cr) over 100 nm thermally grown silicon oxide on silicon wafers and the other consists of 10 nm evaporated Cr over 6 μm polyimide on silicon wafers. The polyimide (Du-Pont PI-2590D) was spun cast at 3,000 rpm and was baked at 170°C for 2 hours before Cr evaporation.

C. Langmuir-Blodgett films

The L-B film depositions were performed using a Joyce-Loebl Langmuir Trough IV equipped with a microbalance for measurement of the surface pressure by the Wilhelmy plate method. Filtered deionized water with a pH of 7 was used for the subphase. PMMA was spread on the water surface from a dilute chloroform solution (~ 10 mg PMMA in 20 ml chloroform). Prior to compression a 20-minute interval was allowed for solvent

evaporation. The Langmuir film was compressed to the transfer pressure (~ 15 dyn/cm) at a rate of 50 cm^2/min, followed by a 20-minute equilibration period. The Cr-coated wafers were immersed into the subphase before the PMMA was spread on the water surface. The first monolayer of PMMA was transferred at the speed of 2 mm/min during the first upstroke of the substrate. After the first monolayer was transferred, baking at 170°C for 20-minutes was performed before subsequent layer transfer. The multilayer films received another baking at 170°C for 20-minutes before electron beam exposure.

D. Electron beam lithography

L-B PMMA films transferred at 15 dyn/cm, with thicknesses between 0.85 nm (one monolayer) and 7.7 nm (9 layer), have been prepared and investigated as high resolution electron beam resists by exposure with a Hitachi S800 scanning electron microscope (SEM), a modified Perkin Elmer MEBES I pattern generation system and a High Resolution Electron Beam Lithography System (HREBLS). The Hitachi S800 exposures used a 0.15 μm beam diameter, 2.5 kV accelerating voltage and 80 pA beam current. Lines were written with a single pass of the electron beam, with doses ranging from 10 - 150 μC/cm^2. The MEBES exposures were performed at a 20 MHz address rate, 10 kV accelerating voltage, 0.125 μm beam diameter and address size, and 6 nA beam current. The HREBLS was designed and built at Stanford for the fabrication and study of microstructures.[10] The exposures in this work used a 8 nm beam diameter, 40 kV accelerating voltage and 3 pA beam current. Lines were written with a single pass of the electron beam, with doses ranging from 0.5 nC/cm to 4.0 nC/cm.

After exposure, the PMMA was developed in a solution of 3:7 cellosolve:methanol for 10 sec. Postbaking at 90°C was performed for 30 min after developing. Following the postbaking process the samples were immersed in a 5:2 deionzed water : Cr etching solution (Cyantek CR-14) for 100 sec to transfer the resist pattern to Cr. After Cr etching the resist was stripped using acetone rinsing. The sample was then examined by SEM.

MONTE-CARLO SIMULATION

The programs used in the Monte-Carlo simulation were derived from a core program by D. C. Joy.[11] The plural scattering approximation described by Bishop[12], Myklebust et al[13] and D.C.Joy[11,14] was adopted as the model for our calculation of the proximity effect on a multilayer substrate. The polynomial extrapolation modification of Love[15] was also adopted for the low energy regime where the Bethe energy loss equation gives unrealistic results. We optimized the empirical parameter introduced by Myklebust in 1976, by matching the computed backscattering yield and experimental data[16,17] and set the modified boundary condition for the plural model of a multilayer substrate according to the method of Hawryluk[18]. Even though models of this type make significant approximations, their accuracy in predicting the backscattering yield and angular energy distribution is reasonably good. Our Monte-Carlo calculations for bulk substrates are in good agreement with the experimental data of Niedrig[16] and Reimer[17] over the range of 5 keV-40 keV beam energies. Our calculation on the backscattering yield and energy absorption distribution for a multi-layer substrate also shows good agreement with other Monte-Carlo calculations and experimental results.(Kyser[19], Hawryluk[20]).

For the calculations reported here, a 100 nm diameter gaussian beam and 2000 trajectories were used. The distribution of energy absorption density in the top layer of the resist film for the backscattered electrons as well as backscattering yield were calculated.

RESULTS

A. Experimental

Figure 1 shows the results of exposure using a MEBES I operating at 10 keV with a 0.125 μm spot and address size. Figures 1a-1e show the patterns produced in 50-nm thick Cr layers using 1, 3, 5, 7 and 9 layer L-B PMMA films as resists, respectively. The substrates of these samples were 50-nm-thick Cr films over 100 nm SiO_2 films on Si wafers. Lines-and-spaces patterns of 0.125 μm have been achieved for all these samples.

Two distributions of porous defects are observed in the Cr films after exposure and etching. The first type is uniform over the sample area and the number of defects increases dramatically with decreasing resist thickness. The second type of defect distribution is close to the exposed regions (within 0.1 μm) and is most easily seen in films thicker than those exhibiting uniform porosity. Figures 2a and 2b are patterns in 50-nm thick Cr films using 7 and 9 monolayer L-B PMMA resists. The patterns were exposed using an Hitachi S800 SEM operating at 2.5 kV accelerating voltage. It can be seen from Figure 2a that the Cr film is porous in the vicinity of the exposure using a 7 layer LB film. This is similar to the deterious effects in the MEBES exposure of the 7 monolayer sample (Figure 1d). However, the density of these defects at the lower accelerating voltage is much higher than that in the sample exposed with MEBES at 10 keV. It can also be seen by comparing Figures 2a and 2b that much poorer line edge definition is seen in the 7 layer sample as compared with that in the 9 layer sample. However, this deterious effect disappeared in the 7 layer sample exposed with the HREBLS at 40 kV accelerating voltage using the same substrate (Cr/SiO$_2$/Si). Figures 3a and 3b are the patterns in 50-nm-thick Cr layers using 7 layer L-B PMMA films as resists exposed with the 40 keV beam. 25-nm-wide lines have been achieved in 50-nm thick Cr for these samples.

Figure 4 shows a pattern of 2 μm deep trenchs in 6-μm-thick polyimide films with a 10 nm thick Cr overcoat. These patterns were fabricated by using a 7 layer L-B PMMA resist exposed with MEBES at 10 keV beam energy. The patterns were transferred into 10-nm Cr and 2 μm polyimide by Cr wet etching and O$_2$ reactive ion etching (RIE), respectively. The second type of defects did not appear in this sample. Cracks, which caused by the internal stress of the thick polyimide layer, are observed.

B. Monte Carlo Simulations

The Monte-Carlo simulation results are shown in Figures 5a-d. The upper plot shows the trajectories of 250 electrons. The bottom plot shows the distribution of the energy

absorption density (erg/cm^2/Coulomb) of the backscattered electrons on a log-scale with distance from the center of a 100 nm gaussian primary beam. For this calculation the PMMA film was divided into 5 layers, and the absorbed energy density was calculated for each layer. The results presented here are from the bottom layer at the Cr interface. The presence of the Cr layer was suspected to influence the exposure of the thin resist films. The backscattering yields from the PMMA and the Cr were therefore calculated seperately. The backscattering yield I is defined as the yield of the backscattered electrons emited from the PMMA surface per primary electron. The backscattering yield II is defined as the yield of backscattered electrons emitted from the Cr surface within a 0.4 μm radius from the center of the beam per primary electron.

In Figure 5 shows the simulated effects of different beam energies and substrate on the backscattering yields. Figure 5a, in which the substrate consists of 50-nm-thick Cr over SiO$_2$ and the primary beam energy is 10 keV, the backscattering yield II is 12.5%. In Figure 5b, in which the same substrate as that of Figure 5a has been used, but with a primary beam energy of 2 5 keV, the backscattering yield II increased to 28.4%, but with a much denser distribution close to the center of the beam. We notice in this case that almost all the backscattered electrons originate from the 50-nm-thick Cr layer. This high backscattering yield can be reduced by either using a higher energy beam or using a substrate consisting of a lower atomic number material. In Figure 5c, in which the substrate is the same as that used in Figure 5a and 5b but with a higher primary beam energy (40 keV), the backscattering yield II was reduced to only 1.2%. In the last case Figure 5d, in which the substrate consists of a 10-nm-thick Cr layer over polyimide and with a 10 keV primary beam, the backscattering yield II is only 0.8%.

A summary of the experimental results, including the simulation calculation, are listed in Table I.

DISCUSSION

We have investigated the lithographic performance of ultrathin PMMA films prepared by L-B technique as high resolution electron beam resists. Even a one monolayer PMMA film (0.85 nm) can act as a positive resist for lithographic processing. However, two types of defects have also been observed as shown in Figures 1a-d. The first type of defect which increased in density uniformly across the sample as the film thickness decreased, is possibly due to an intrinsic weak spot in the resist films. As the film thickness increases, this type of defect can be covered up by the next layer above it. This defects have an estimated size of less than 20 nm in diameter. This area is approximately the total area of 2,500 PMMA repeat units (each repeat unit is ~0.16 nm^2), which by coincidence this is about the same of the size of PMMA we used in this study (1,881 repeat units).

The second kind of defect, which only appears in proximity to the exposed region, is probably related to the electron-resist interactions. From Table I we know these defects occur in films thinner than 9 layers for exposure with both the 2.5 keV and 10 keV beam energies. For a proximity effect related to backscattering this is surprising. The backscattered electrons will return to the surface with an average energy about one half of the primary beam energy,[21] and these backscattered electrons should travel through both the 7 and 9 layer PMMA films. The thickness difference between 7 layer and 9 layer PMMA films is only about 1.7 nm. It would seem unlikely that the deterious effect we have seen is directly related to the backscattered electrons. From Table I we also notice that this type of defect does not appear in the 10 keV MEBES exposed 7 layer PMMA films when the 50 nm Cr/ 100 nm SiO_2 substrate was replaced by the 10 nm Cr/ 6-μm-thick polyimide layer or in the 40 keV HREBLS exposed 7 layer PMMA films using 50 nm Cr/ 100 nm SiO_2/ Si substrate. From the Monte-Carlo simulation, we know that either replacing the substrate with thin Cr and thick polyimide layers for 10 keV exposure or using 50 nm Cr/ 100 nm SiO_2/ Si substarte for 40 keV exposure reduce the backscattering yield from 16.8 % to 0.8% or 1.2%, respectively. Therefore, reducing the backscttered

electrons can minimize those defects around the exposed region, even though the backscattered electrons are not directly related to this deterious effect. Furthermore, these defects are distributed more closely to the patterns in the 2.5 keV exposed sample than in the 10 keV exposed sample. Based on these results, a possible explanation is proposed for the formation of these defects.

These defects are possibly caused by the exposure of secondary electrons, which are generated by the backscattered electrons at the Cr surface as shown in figure 6a. Generation of secondary electrons have also been reported by Allen et al.[22] for a different system. They reported a Monte Carlo calculation of low-energy electron emission from sufaces and predicted that the secondary electrons (< 50 eV), generated by the backscattered electrons have almost the same yields per unit area as a function of distance from the point of impact for primary electrons of energy ~ 3 keV. Furthermore, Broers[23] has suggested the scattering range of the secondary electrons is approximately 6 nm in PMMA, which is similar to the thickness of a 7 layer LB PMMA film (6 nm). It is possible therefore that the exposure effect of these secondary electrons will only be observed for films with less than or equal to 7 layers of PMMA.

In figures 6b we have shown the energy dissipated by the secondary electrons per unit volume, generated by the backscattering electrons, as a function of resist layers. In figure 6c and 6d we have plotted the distribution of the total energy dissipated in the top layer of a 7 and 9 layer resist, respectively. In the case of the 7 layer exposure, the shape of the total energy dissipated due to the effect of secondary electrons is broadened relative to that of the 9 layer case. We should expect a much lower image contrast in the case of 7 layer exposure, and that's what is observed by comparing Figures 1d and 1e, and Figures 2a and 2b. By reducing the backscattered electrons, either by using a high energy beam or a substrate with low atomic number, one can reduce the effect of these secondary electrons and therefore reduce the deterious effect. Our Monte-Carlo calculations on the backscattering yield are consistent with the experimental observations.

These results show that the resists of thickness less than 6 nm (7 layer) will be exposed by the secondary electrons. This strongly supports the resolution limit (12 nm) in electron beam lithography proposed by Broers[23] for thin substrates. Broers has suggested that the resolution is set by the range over which the primary electrons interact with the resist. This range is the distance over which the low energy secondary electrons are created and by the range of the secondaries in the resist.

SUMMARY

We have observed that a one monolayer PMMA (0.85 nm) film can act as a positive electron beam resist for lithographic processing. A proximity effect has been reported for the exposure of PMMA resist films thinner than 7.7 nm (9 layers). This is contributed by the secondary electrons generated by the backscattered electrons at the resist-substrate interface. This local effect can be minimized by using a substrate with lower atomic number or using higher energy beams. We also report a different type of defect generated by the weak spot in the L-B PMMA films. This defect decreases dramatically as the film thickness increases. Further studies on this intrinsic defect is suggested.

ACKNOWLEDGMENTS

REFERENCES

a.   Presently with LSI R&D Laboratory, Mitsubishi Electric Corporation, Itami , Japan.

1.   T. H. P. Chang and A. D. G. Stewart, *Proc. 10th Symp. on Electron, Ion and Laser Beam Technology*, edited by L. Marton (San Francisco: IEEE, 1969), 97-106.

2.   M. Parikh, J. Appl. Phys. **50**, 6, 4371 (1979).

3.   N. D. Wittels and C. I. Youngman, *Electron and Ion Beam Science and Technology, Eighth International Conference*, edited by R. Bakish (The Electrochemical Society: New York, 1978), 361.

4.   G. Owen and P. Rissman, J. Appl. Phys. **54**, 3573 (1983).

5.   G. A. C. Jones, S. Blythe, and H. Ahmed, J. Vac. Sci. Technol. **B5**, 120 (1987).

6.   Z. W. Chen, G. A. C. Jones, and H. Ahmed, J. Vac. Sci. Technol. **B6**, 2009 (1988).

7.   A. S. Gozdz and P. S. D. Lin, *Proc. SPIE, Symposium on Microlithography*, **923**, 172-177 (1988).

8.   S. W. J. Kuan, C. W. Frank, C. C. Fu, D. R. Allee, P. Maccagno, R. F. W. Pease, J. Vac. Sci. Technol. **B6**, 2274 (1988).

9.   S. W. J. Kuan, P. S Martin, C. W. Frank, and R. F. W. Pease, Proceedings of SPIE 1989, Advances in Resist Technology and Processing, to be published.

10. J. H. Newman, K. E. Williams, and R. F. W. Pease, J. Vac. Sci. Technol. **B5**, 88 (1987).

11. H. E. Bishop, National Bureau of Standards, Spec. Publ. **460**, 5 (1976).

12. R. L. Myklebust, D. E. Newbury and H. Yakowitz, National Bureau of Standards, Spec. Publ. **460**, 105 (1976).

13. D. C. Joy, J. Microscopy **147**, 51 (1987).

14. S. Luo and D. C. Joy, Scanning Microscopy **2**, 1901 (1988).

15. G. Love, M. G. Cox and V. D. Scott, J. Phys. D, **11**, 7 (1978).

16. H. Niedrig, Scanning **1**, 17 (1978).

17. L. Reimer and C. Tollkamp, Scanning **3**, 35 (1980).

18. R. J. Hawryluk, A. M. Hawryluk and H. I. Smith, J. Appl. Phys. **53**, 5985 (1982).

19. D. F. Kyser and K. Murata, National Bureau of Standards, Spec. Publ. **460**, 129 (1976).

20. R. J. Hawryluk, A. M. Hawryluk and H. I. Smith, J. Appl. Phys. **45**, 2551 (1974).

21. H. E. Bishop, Br. J. Appl. Phys. **18**, 703 (1967).

22. T. E. Allen, R. R. Kunz, and T. M. Mayer, J. Vac. Sci. Technol. **B6**, 2057 (1988).

23. A. N. Broers, J. Electrochem. Soc. **128**, 166 (1981).

TABLE I Summary of the experimental and simulation results

| Samples	Second type of defects	Backscattering Yield	
		I	II
3 layers PMMA/50 nm Cr/ 100 nm SiO_2/Si			
10 keV beam exposure	Yes	19.8%	12.5%
5 layers PMMA/50 nm Cr/100 nm SiO_2/Si			
10 keV beam exposure	Yes	19.8%	12.5%
7 layers PMMA/50 nm Cr/100 nm SiO_2/Si			
2.5 keV beam exposure	Yes	27.0%	28.4%
10 keV beam exposure	Yes	19.8%	12.5%
40 keV beam exposure	No	10.5%	1.2%
9 layers PMMA/50 nm Cr/100 nm SiO2/Si			
2.5 keV beam exposure	No	27.0%	28.4%
10 keV beam exposure	No	19.8%	12.5%
7 layers PMMA/10 nm Cr/ 6 μm polyimide/Si			
10 keV beam exposure	No	3.0%	0.8%

042602 25KV X3.00K 10.0um
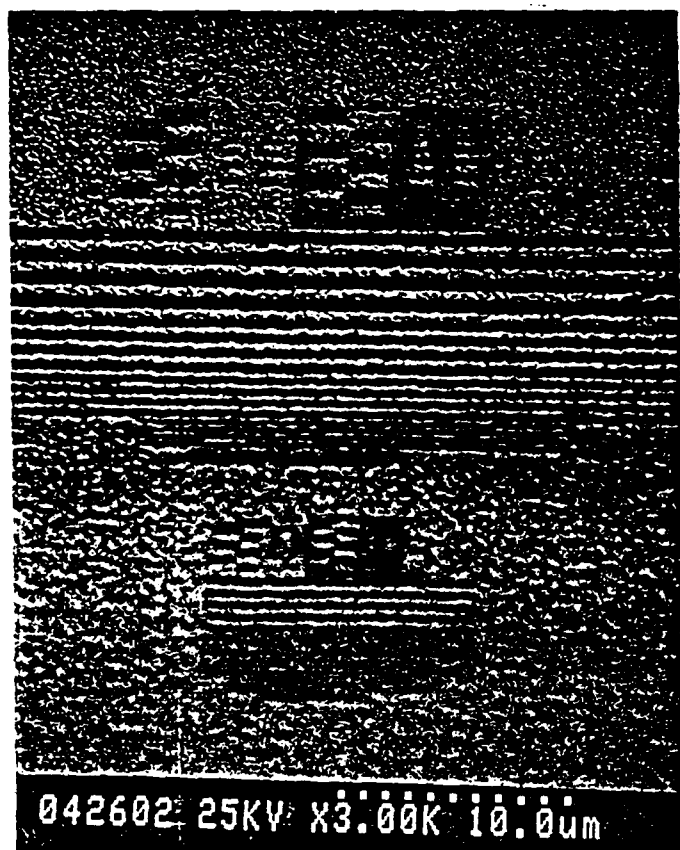
(a)

Figures 1a-e. Patterns etched in 50-nm-thick Cr using 1, 3, 5, 7, and 9 layer L-B PMMA films as resists, respectively, exposed with a MEBES I system operating at 10 kV accelerating voltage, 1/8 μm beam diameter and address size, 6-nA beam current, and with a dose of 100 μC/cm^2. The substrates consisted of 50-nm-thick Cr over 100 nm SiO$_2$ on Si wafers.
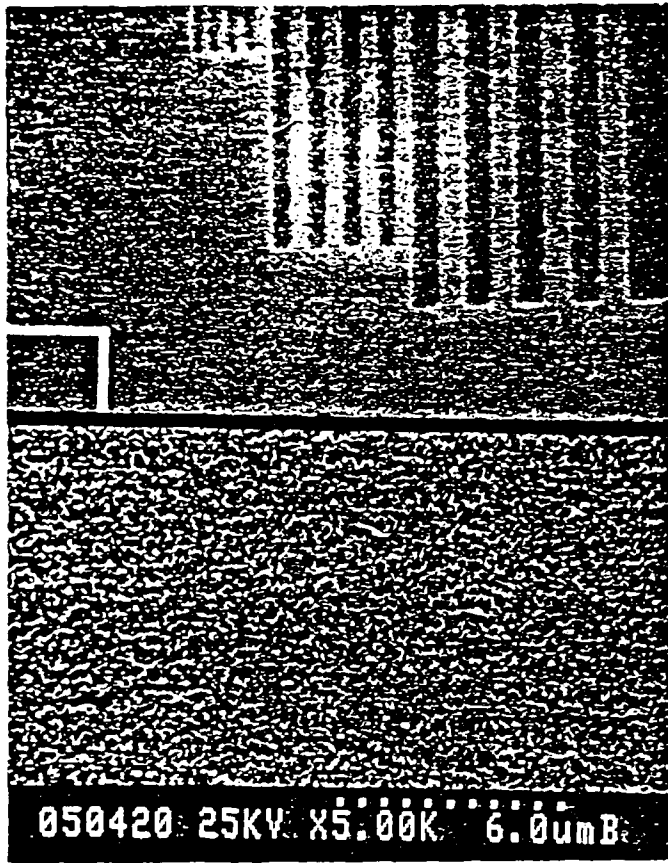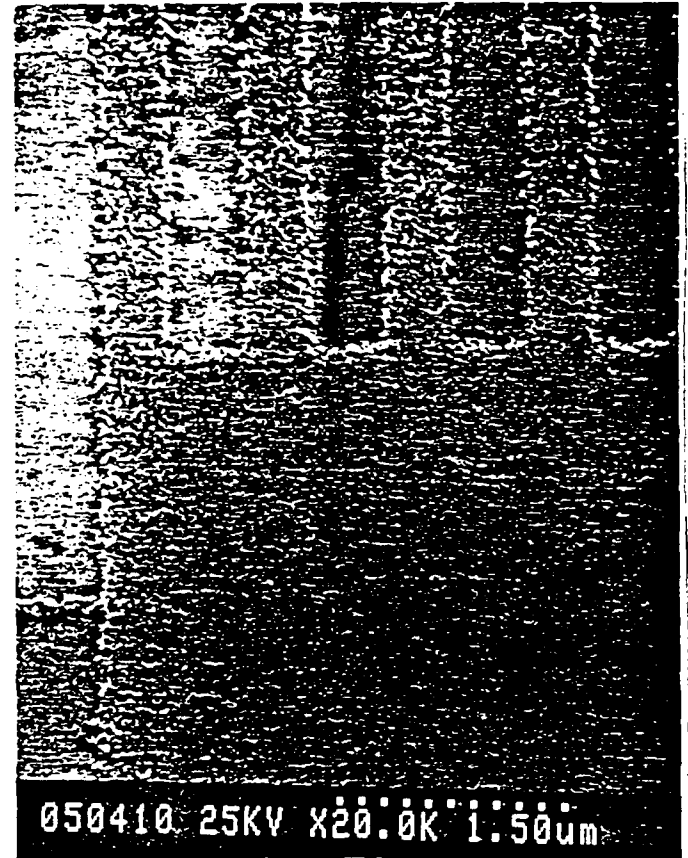
(b)   (c)

Figures 1a-e. Patterns etched in 50-nm-thick Cr using 1, 3, 5, 7, and 9 layer L-B PMMA
films as resists, respectively, exposed with a MEBES I system operating at 10 kV
accelerating voltage, 1/8 μm beam diameter and address size, 6-nA beam current, and with
a dose of 100 μC/cm^2. The substrates consisted of 50-nm-thick Cr over 100 nm SiO$_2$ on
Si wafers.
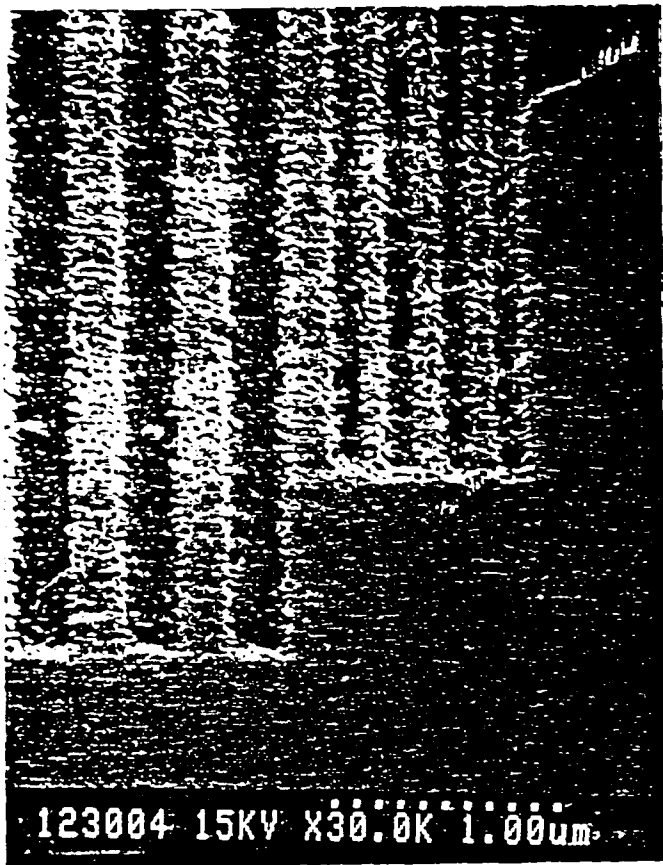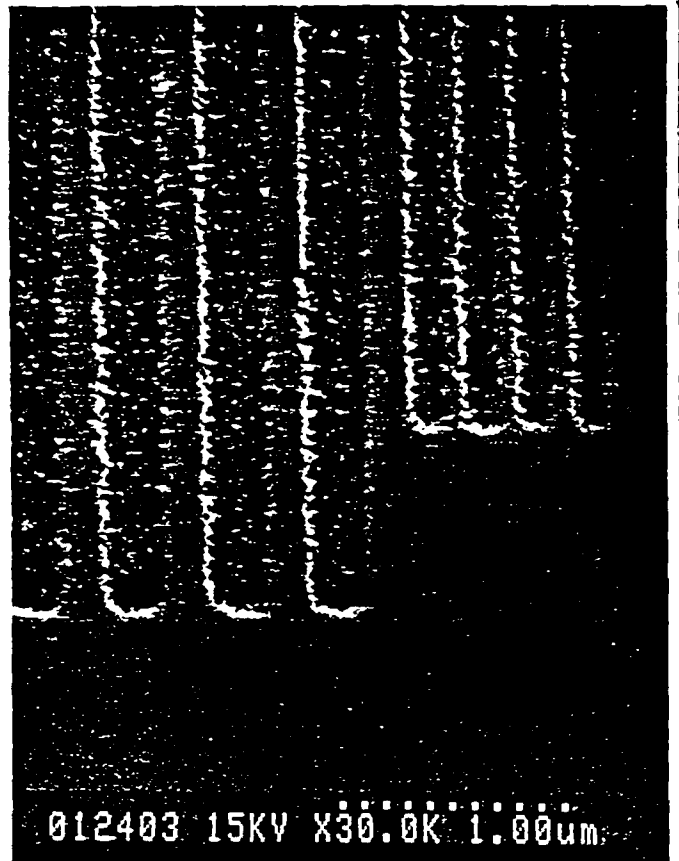
(d) (e)

Figures 1a-e. Patterns etched in 50-nm-thick Cr using 1, 3, 5, 7, and 9 layer L-B PMMA films as resists, respectively, exposed with a MEBES I system operating at 10 kV accelerating voltage, 1/8 μm beam diameter and address size, 6-nA beam current, and with a dose of 100 μC/cm². The substrates consisted of 50-nm-thick Cr over 100 nm SiO₂ on Si wafers.
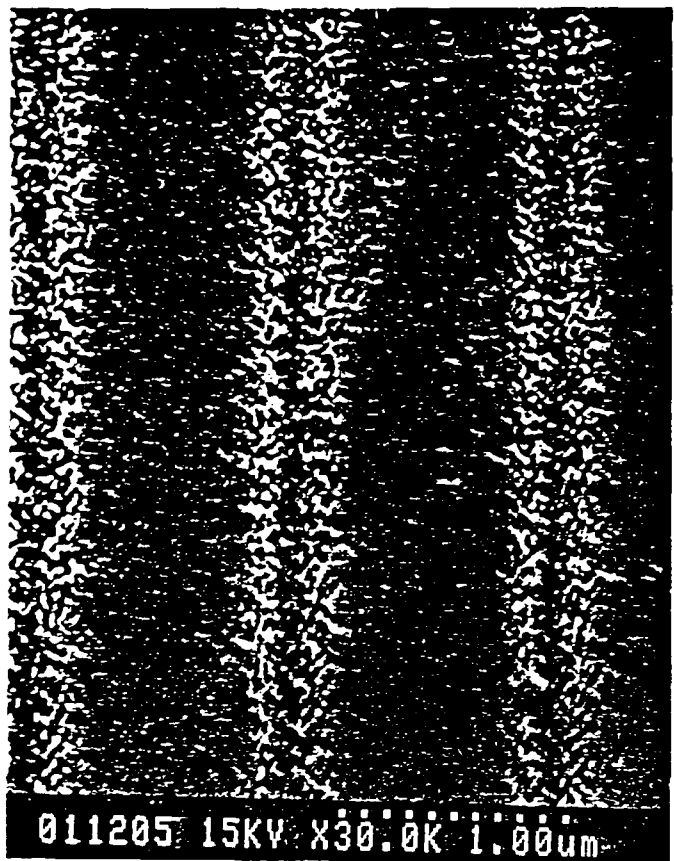
(a)
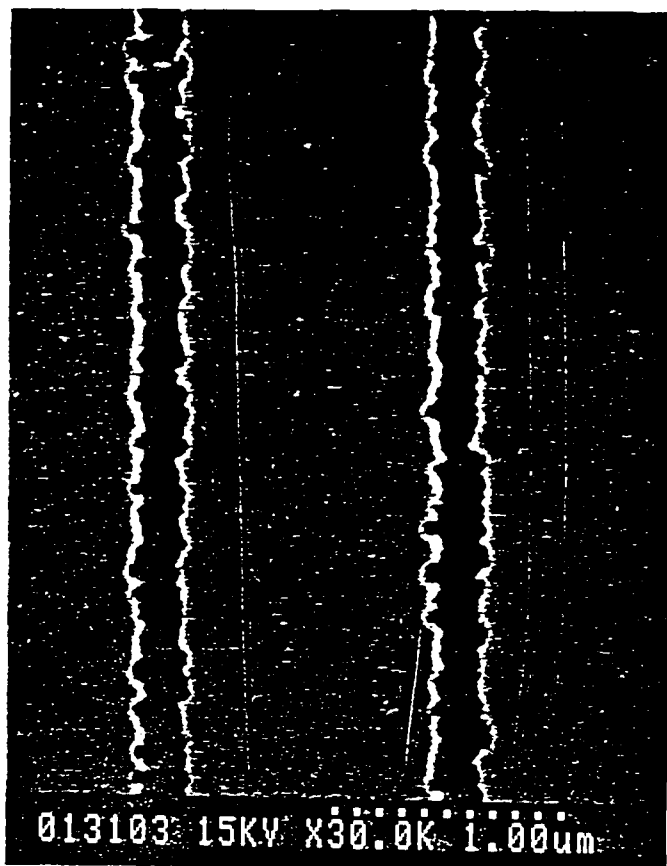
(b)

Figures 2a-b. Patterns etched in 50-nm-thick Cr using 7 and 9 layer L-B PMMA films as resists, respectively, exposed with a Hitachi SEM operating at 2.5 kV accelerating voltage, 0.15 μm beam diameter, 80 pA beam current , and with a dose of 50 $\mu C/cm^2$. The same substrates as the ones described in Fig. 1 were used.
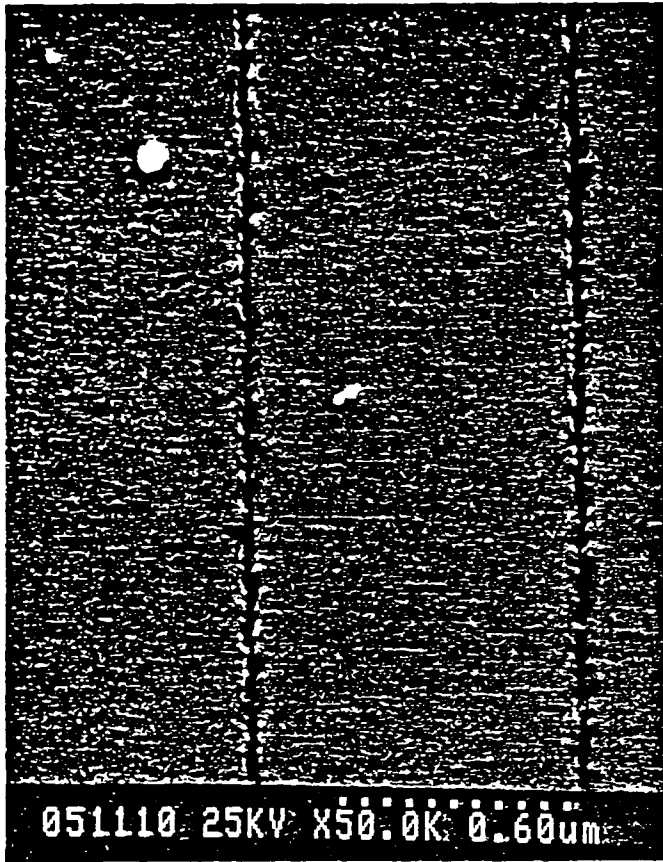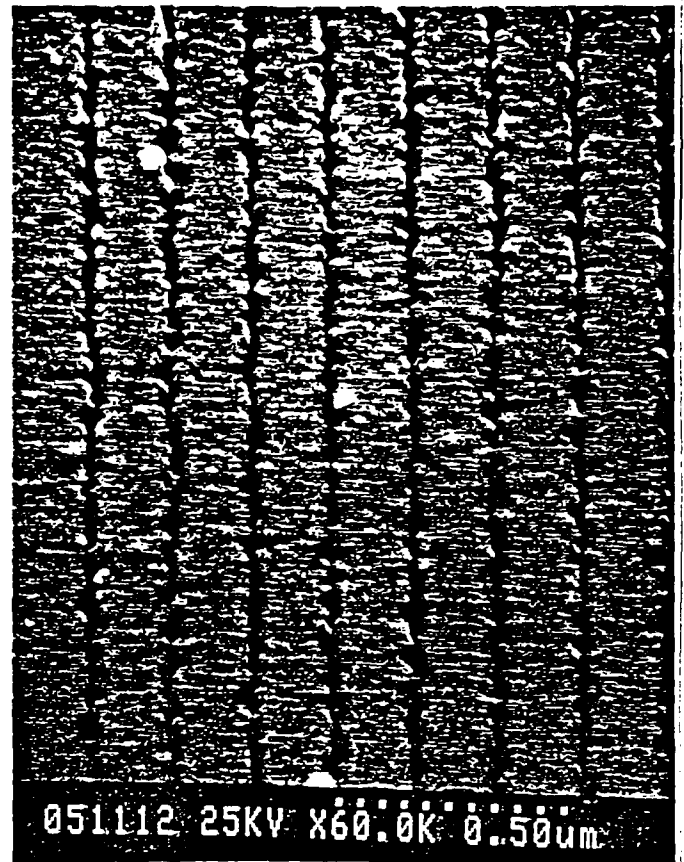
(a)   (b)

Figures 3a-b. Patterns etched in 50-nm-thick Cr using 7 layer L-B PMMA films as resists, exposed with a high-resolution lithography system operating at 40-kV accelerating voltage, 8 nm beam diameter, 3-pA beam current and with a dose of 200 $\mu C/cm^2$. The lines etched in 50-nm-thick Cr are only 25 nm wide. The same substrates as the ones described in Fig. 1 were used.

Figure 4. Patterns etched into 6 μm polyimide by oxygen RIE using 10-nm-thick Cr as the mask. The patterns in Cr were patterned with a 7 layer L-B PMMA film as resist, exposed with a MEBES I system operating at 10 kV accelerating voltage, 1/8 μm beam diameter and address size, 6-nA beam current, and with a dose of 100 μC/cm^2. The substrates consisted of 10-nm-thick Cr over 6 μm polyimide on Si wafer.

(a)

(1) Energy = 10 KeV

PMMA	100A
Cr	500A
SiO2	
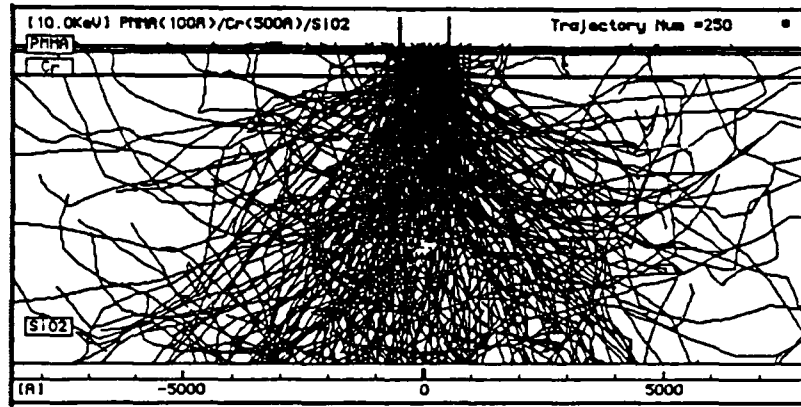
(2) Backscattering yield

BS- I	19.8%
BS- II	12.5%
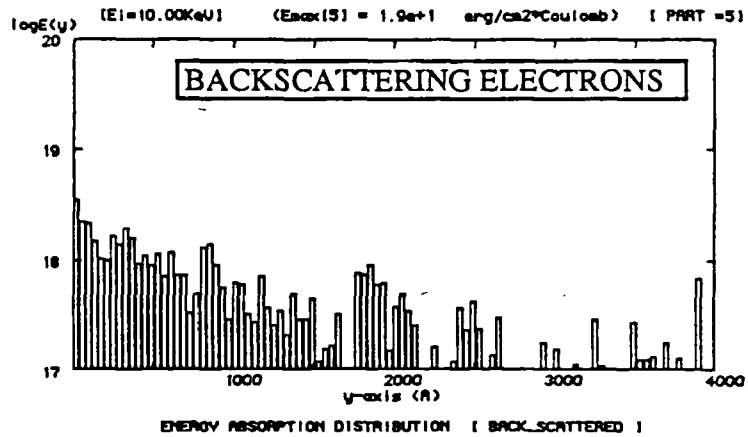
(b)

(1) Energy = 2.5 KeV

PMMA	100A
Cr	500A
SiO2	
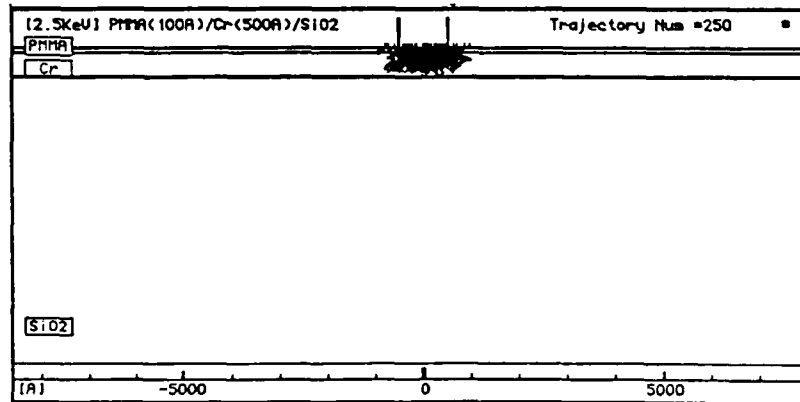
(2) Backscattering yield

| BS- I	27.0%
BS- II	28.4%
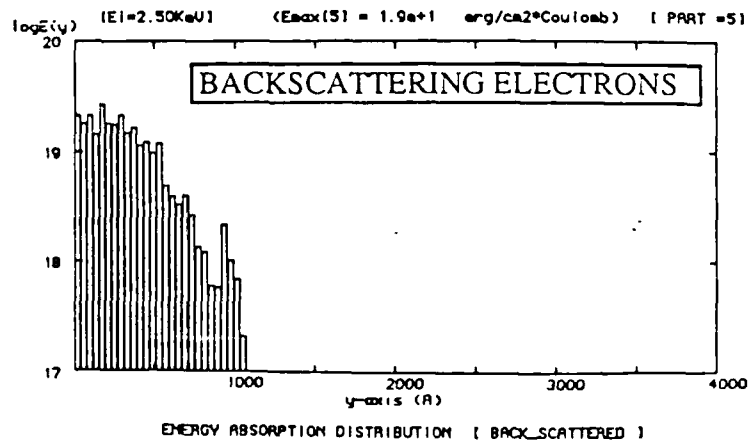
Figure 5A-B. Trajectory plot of 250 electrons(1) and the distribution of energy absorption density of backscattering electrons(2). 2000 electrons are used in (2).

(c)

(1) Energy = 40 KeV

PMMA	100A
Cr	500A
SiO2	
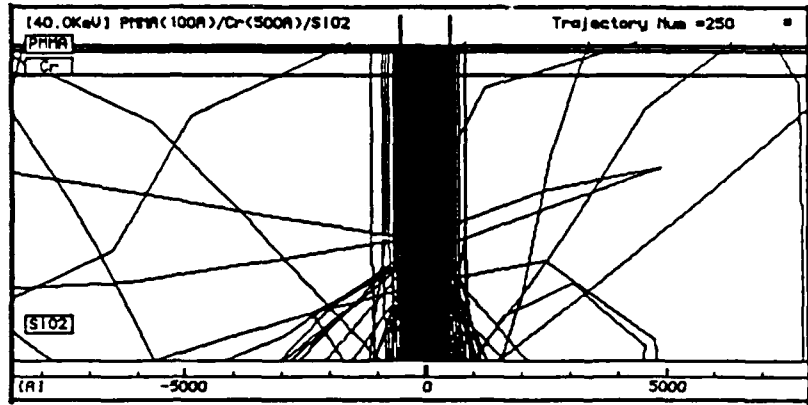
(2) Backscattering yield

BS- I	10.5%
BS- II	1.2%

NOTE ==>>
LONG RANGE (E14-E20)

[40.0KeV] PMMA(100A)/Cr(500A)/SIO2　　Trajectory Num =250

PMMA
Cr
SIO2

[A]　　　　-5000　　　　0　　　　5000

logE(y)　[EI=40.00KeV]　(Emax(5) = 1.7e+1　erg/cm2*Coulomb)　[PART =5]

BACKSCATTERING ELECTRONS

y-axis (A)

ENERGY ABSORPTION DISTRIBUTION　[BACK_SCATTERED]

(d)

(1) Energy = 10 KeV

PMMA	100A
Cr	100A
POLYIMID	

[10.0KeV] PMMA(100A)/Cr(100A)/POLYIMID　　Trajectory Num =250

PMMA
Cr
POLYIMID

[A]　　　　-5000　　　　0　　　　5000

logE(y)　[EI=10.00KeV]　(Emax(5) = 1.8e+1　erg/cm2*Coulomb)　[PART =5]
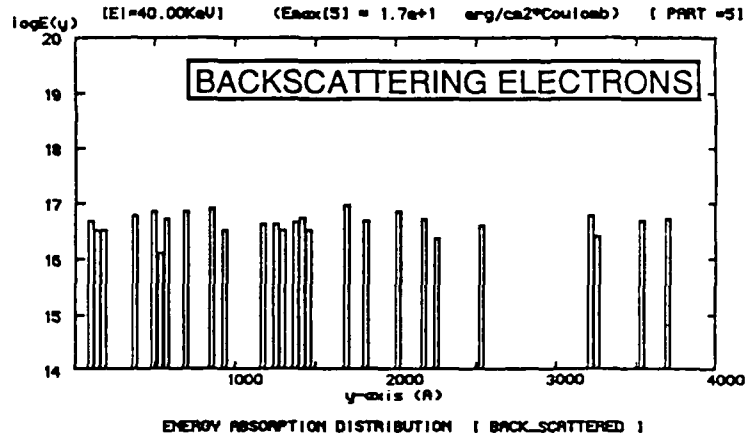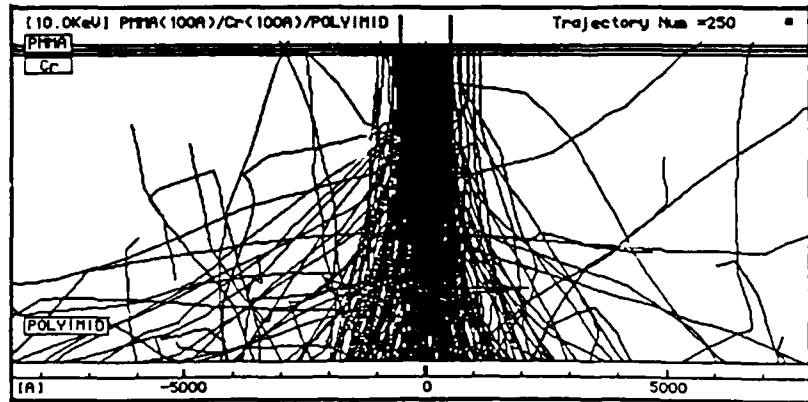
(2) Backscattering yield

BS- I	3.0%
BS- II	0.8%

y-axis (A)

ENERGY ABSORPTION DISTRIBUTION　[BACK_SCATTERED]
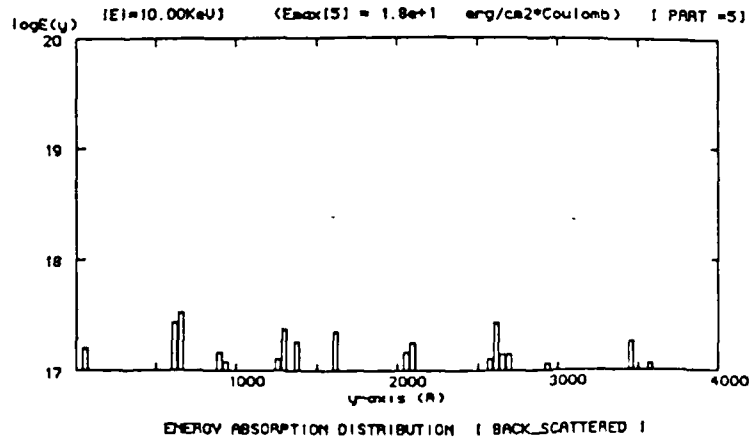
Figure 5C-D. Trajectory plot of 250 electrons(1) and the distribution of energy absorption density of backscattering electrons(2). 2000 electrons are used in (2).

Primary Electrons

Backscattered Electrons

● **Secondary Electrons**

**LB PMMA Films**
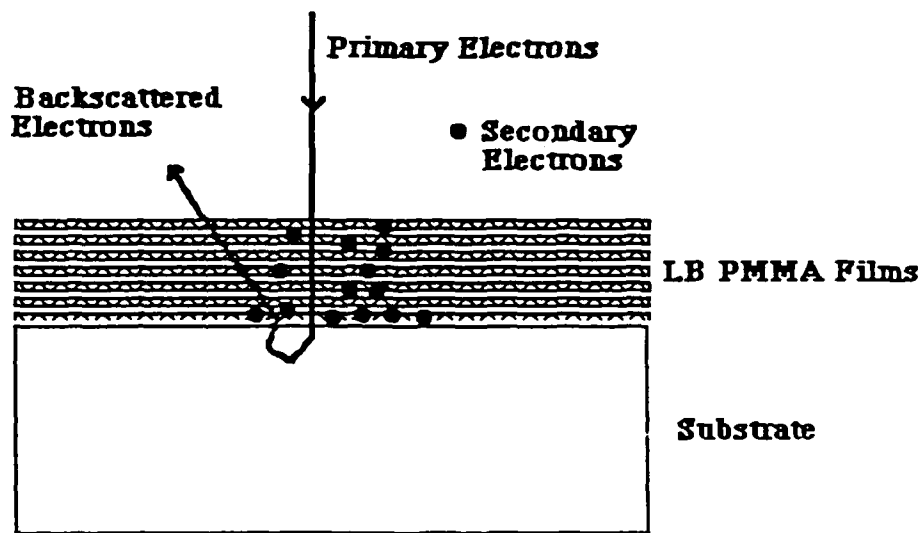
Substrate

(a)

Figure 6a. Schematic of the interactions between electrons and resist on the solid substrate.

Energy Dissipated by the Secondary Electrons/ Unit Vol.
(generated by the backscattered electrons)


7   9

Number of Layer
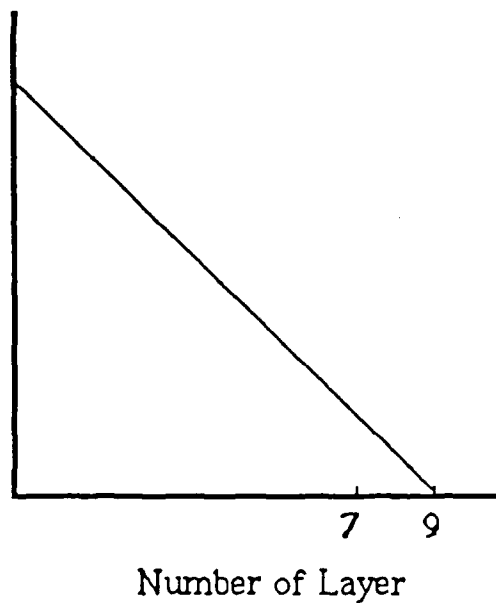
(b)

Figure 6b. Energy dissipated by secondary electrons which generated by the backscattered electrons per unit volume as a function of film thickness.

Energy Dissipated
by Primary Electrons

Total Energy Dissipated

Energy Dissipated by
Backscattered Electrons

0.1 μm

Energy Dissipated by
Secondary Electrons
(Generated by Backscattered Electrons)

(c)

Total Energy Dissipated
without the Effect of
Secondary Electrons

0.1 μm
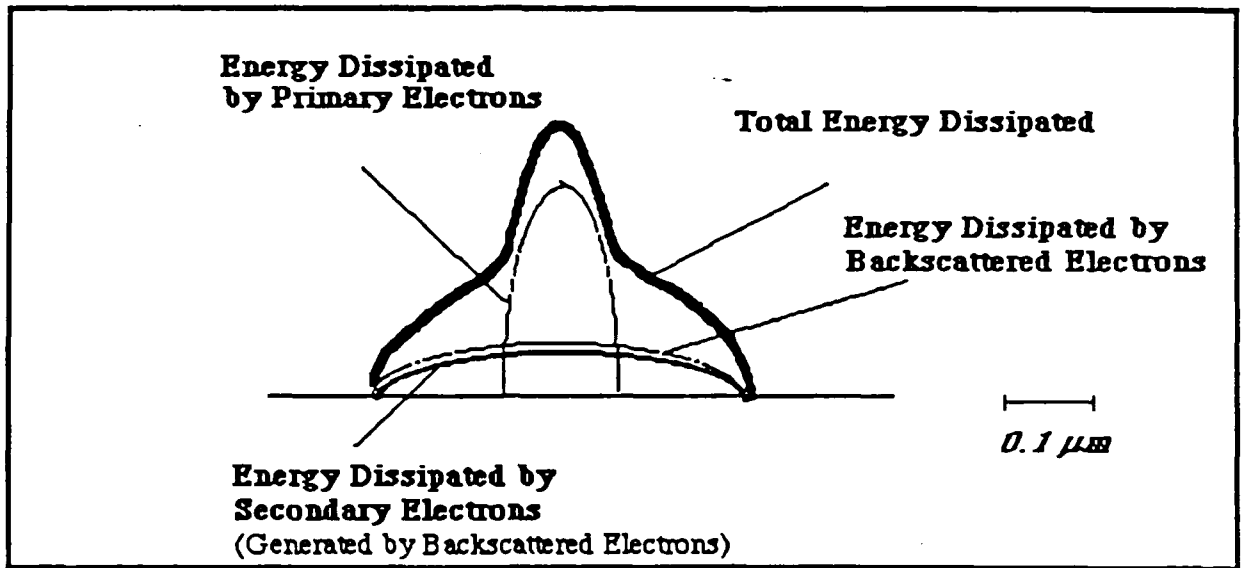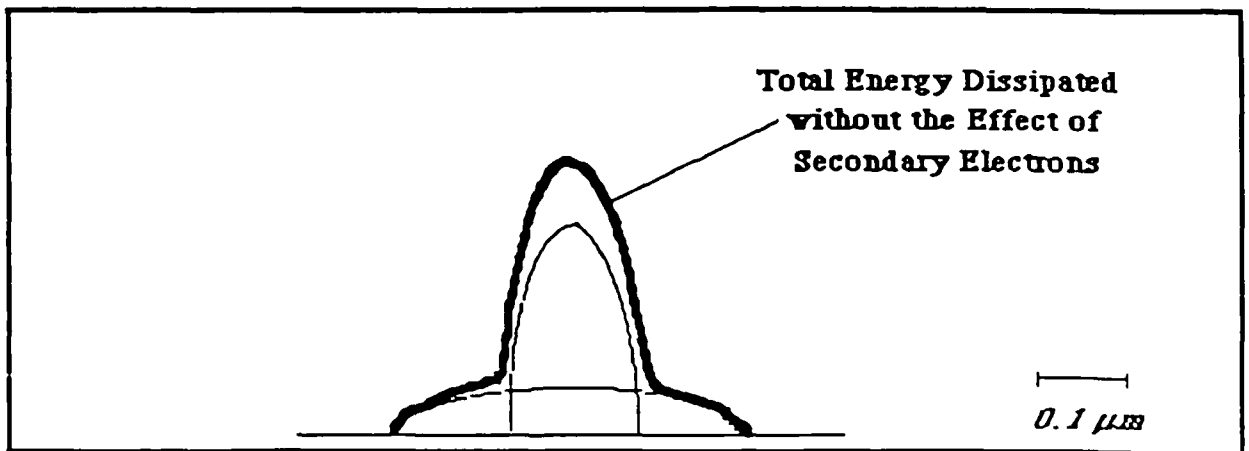
(d)

Figure 6c-d.   Schematic distribution of the total electron energy dissipated in the top layer
of the 7 layer and 9 layer L-B PMMA resists films, respectively.